

Chapter 6

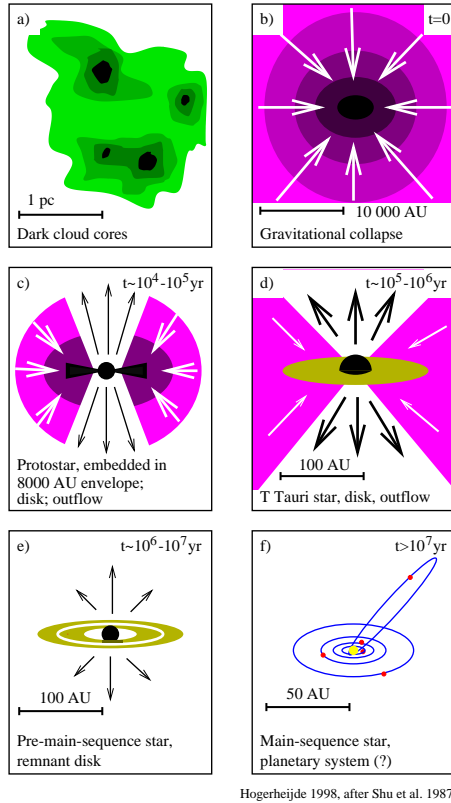
Concluding remarks and suggestions for future work

Abstract

Circumstellar disks similar to models of the solar nebula have now been detected around several stars with masses comparable to our sun ($0.2\text{--}10 M_{\odot}$) and, as I have discussed in this thesis, are a good environment in which to address the question of planet formation. As analogs to the solar nebula, circumstellar disks offer a unique opportunity to study the conditions during the star and planet formation process. The assessment of the chemical composition in these disks can provide valuable information (i.e., density, thermal history and composition) about the initial conditions in planet-forming zones, in the solar nebula and in exoplanetary systems, and help to determine the origin of primitive bodies such as comets. While disk structure is complex, when observed at sufficient spatial and spectral resolution molecular lines can be used to probe the effects of UV fields, temperature variations, ionization and grain-surface reactions on the composition of the gas. Studies of the grain composition and grain surface reactions are also very important, as current models of the chemistry in the outer regions of circumstellar disks (Aikawa et al., 2002; Willacy & Langer, 2000; Finocchi et al., 1997; Bauer et al., 1997) suggest that at large radii the chemistry is highly affected by adsorption onto and desorption from grains. Grains also play a large role in determining the temperature structure and geometry of disks, through reprocessing of stellar radiation. The interpretation of the observed molecular line emission and comparison with chemical models requires knowledge of molecular excitation and disk radiative transfer. Through the comparison of the chemical abundances in circumstellar disks with those of other YSOs, changes in the physical structure during the process of star and planet formation can be monitored. Here I summarize briefly what is known about the evolution of molecular complexity in star and planet formation before turning to an assessment of future observations and modeling of circumstellar disks.

6.1 Chemistry as a function of star formation

Interstellar dust, gas and ice are the building blocks of stars, planets and comets. Modification of this material during the star formation process is believed to result in complex chemical networks in the gas phase and in ices on grain surfaces. The desorption of these ices in turn enhances the complexity of gas-phase chemistry. Interstellar materials are precursors to that in circumstellar disks, similar to our own solar nebula, in which the planets and comets were formed. The material in the outer radii of these disks is relatively unprocessed and similar to its interstellar origin, while material near the star has been significantly modified by the star formation process. Thus, observations tracing the evolution of material in young stellar objects (YSOs) are essential for addressing issues such as the formation of comets and the origin of life.



Hogerheijde 1998, after Shu et al. 1987

Figure 6.1 The star and planet formation process (Hogerheijde, private communication, 1998). Interstellar gas and dust condenses into dense cores, shielding the enclosed gas and dust from interstellar radiation and allowing the buildup of ices on dust surfaces. Collapse ensues and a star is born in the center of the core, heating and processing the material in the surrounding envelope. Dust and gas accretes onto the star through a circumstellar disk and a bipolar outflow sweeps out surrounding gas. The grain mantle ice may be processed by shocks in this outflow, but remains pristine in the outer, quiescent parts of the disk. The solar system produced will show evidence of the star formation process in the composition of its planets, meteorites and comets.

A diagram of the star formation process is presented in Figure 6.1. At the low temperatures of dense molecular cores ($T = 10\text{--}40 \text{ K}$; $n = 10^2\text{--}10^6 \text{ molecules/cm}^3$), gaseous species (atoms and molecules) rapidly accrete onto grain surfaces at roughly the collision rate forming ice mantles that are on the order of $1 \mu\text{m}$ thick. Laboratory experiments indicate that C, N, O atoms and H_2 can hop across grain surfaces and hydrogen and deuterium atoms tunnel through barriers, scanning the entire grain surface in $\sim 10^{-7}\text{s}$. Thus, hydrogenation is efficient on these cold grains and laboratory studies confirm that H_2 , NH_3 , CH_4 and H_2O are indeed produced in such environments. CO and

H_2 , once formed, are self-shielding, and CO is the most abundant observable molecule by 3 orders of magnitude in these cores. This does not imply chemical simplicity, however, as long carbon-chain molecules have been observed toward even the youngest cores, i.e., TMC-1 (Kawaguchi et al., 1992; Takano et al., 1998). The carbon-chain molecules C_2S and HC_3N were found to be correlated with each other, but not with NH_3 nor N_2H^+ and the $\text{C}_2\text{S}/\text{N}_2\text{H}^+$ or $\text{C}_2\text{S}/\text{NH}_3$ ratios have been used as indicators of the amount of time since the gas was atomic-carbon rich (Bergin & Langer, 1997).

The star formation process continues with collapse of the dense core and the newborn star will heat the surrounding material, leading to desorption of grain-mantle ices and enrichment of the gas-phase chemistry. Systematic observations of molecules other than CO have been pursued only for a few low mass sources during the collapse (or Class 0) stage, the most notable of which is IRAS 16293-2422 (Table 6.1). For this source, large chemical gradients have been seen, with organics such as CH_3OH and CH_3CN in warm, inner parts of the envelope, while the edge of the envelope is dominated by optically thick HCO^+ , N_2H^+ and HNC (van Dishoeck et al., 1995). Recent studies indicate that the chemical composition in the inner regions is quite similar to that seen in hot cores around high-mass stars (Schöier et al., 2002). Due to efficient desorption of grain mantles, fully hydrogenated molecules, such as H_2O , NH_3 , H_2S and CH_3OH are very abundant in hot cores. Because sulfur is effectively locked up as H_2S on grain surfaces in cold clouds, the abundance of S-bearing molecules in general is much higher in hot cores (2–3 orders of magnitude higher than in earlier stages; see Table 6.1) as well, and the relative abundances of S-bearing molecules has been used as a “chemical clock” to monitor the thermal desorption process and the time elapsed since warming began. The chemistry of ices in this stage can also be enriched by energetic processing, such as ultraviolet irradiation and cosmic rays. Laboratory UV photolysis of “astronomical,” methanol-containing ices produce a variety of complex molecules, including alcohols, nitriles and isonitriles, hexamethylenetetramine (HMT), polyoxymethylene (POM), amides and ketones on grain surfaces (Allamandola et al., 1999; Bernstein et al., 1995). Species such as alcohols and ethers, and molecules as complex as glycolaldehyde (Hollis et al., 2000) have been observed in hot cores, indicating that energetic processing of grains may provide a facile route to the development of prebiotic molecules.

As infall continues, a disk forms around the star and an outflow develops perpendicular to the plane of the disk. The outflow clears a cavity in the core and reveals warm dust close to the forming star. In such Class I objects, the high densities and velocities within the outflow in this phase lead to increased collisions between grains resulting in the continued evaporation of ices from grain mantles and additional sputtering of metals from grain cores. For this reason, the outflows of Class I YSOs are characterized by gas-phase emission from the species mentioned above as well as from molecules which require atoms located in grain cores, such as SiO . Gas-phase abundances for the well monitored class I object L1157 are presented in Table 6.1. In comparison with IRAS 16293-2422, L1157 possesses higher abundances of SiO , S-bearing molecules, and organics such as CH_3OH and

H_2CO as predicted for the above scenario.

As the outflow continues, the outer envelope begins to clear ($\sim 10^6$ yr) and the star becomes visible. The SED at this stage is characterized by emission from the star in the optical and UV and radiation from circumstellar dust at $\lambda > 1 \mu\text{m}$ (Class II). The objects for which we obtained gas-phase abundances reside in this category (and are discussed thoroughly in this thesis and reviewed below). The observed abundances for the class II T Tauri star LkCa 15 are presented in Table 6.1¹. The abundances are in general lower than those observed for L1157, which (as discussed below) is likely indicative of the quiescent nature of the disk, but higher than for IRAS 16293-2422, indicating that desorption from grain mantles is still important.

Comets are the most volatile-rich and pristine objects in the solar system. The composition of comets is expected to be similar to that of the early solar nebula (at $R \sim 30$ AU). Observations of comets probe the comae during close approaches to the Sun and therefore the chemistry observed may be altered from the original abundances (or even core abundances). Models of gas-phase chemistry (Charnley et al., 2002) are usually used to infer parent molecule abundances in the nucleus, but there are several uncertainties associated with doing so. In accordance with this, the abundances measured in comets appear to be similar to, those observed in (the outer radii of) disks, with the exception of molecules formed on grain mantles, such as CH_3OH , H_2CO and the S-bearing molecules, which are likely larger in comets due to outgassing upon approach to the Sun.

6.2 Understanding the physical properties of disks through molecular line observations

As the second most abundant molecule, next to molecular hydrogen, CO is a useful tracer of the physical structure of circumstellar disks. Via comparison with models, or through examination of the data itself, CO emission is often used to constrain the disk size, inclination and rotation axis and velocity. Due to optical depth effects, however, recent studies (Qi et al., 2003) indicate that CO emission is not a good probe of the total disk mass, although this is a common practice (using a conversion of $[\text{CO}]/[\text{H}_2] = 10^{-4}$). Observations of multiple CO transitions can also provide information about the temperature structure in the disk (see Chapter 2; van Zadelhoff et al., 2001). In this study, we use a non-LTE Monte Carlo radiative transfer model (Hogerheijde & van der Tak, 2000) and a physical disk model based on D'Alessio et al. (2001) to simulate molecular line emission from the T Tauri star disk LkCa 15. After using the CO 2-1 transition to constrain the disk structure, these models were used to solve the radiative transfer and molecular excitation for the observed 1-0 transitions of ^{13}CO , C^{18}O , HCO^+ , H^{13}CO^+ and N_2H^+ . The results indicated that the assumption

¹For reasons discussed in Chapter 2 and Qi et al. (2003), this refers to abundances in the warm surface layer at $R \sim 300$ AU and not the total column.

Table 6.1. Fractional abundances in YSOs and comets (adapted from Schöier et al., 2002)

Species	Comets Hale-Bopp ^a	Disks LkCa 15 ^b	Class I L1157 ^c	Hot cores Orion ^d	Class 0 IRAS 16293-2422 ^e
CO	1(-5)	1(-4)	1(-4)	1(-4)	4(-5)
H ₂ O	5(-5)	<9(-4)	...	>1(-5)	...
HCN	1(-7)	1(-7)	5(-7)	4(-7)	1(-9)
CN	...	6(-9)	5(-8)	...	8(-11)
HNC	2(-8)	<3(-10)	5(-8)	...	3(-8)
HCO ⁺	...	5(-10)	3(-8)	1(-9)	8(-9)
CH ₃ OH	1(-6)	5(-8)	2(-5)	2(-7)	3(-7)
H ₂ CO	5(-7)	(0.4-1)(-9)	3(-7)	1(-8)	6(-8)
CS	5(-8)	1(-9)	2(-7)	1(-7)	2.5(-9)
SO	1(-7)	<3(-9)	3(-7)	5(-8)	3.5(-9)
SO ₂	1(-7)	<4(-9)	5(-7)	6(-8)	2(-10)
OCS	2(-7)	<42(-9)	2(-7)	5(-8)	<3(-9)
H ₂ S	7(-7)	<4(-8)	4(-7)	<1(-7)	...
SiO	...	<1(-10)	7(-8)	6(-8)	2.5(-11)

Note. — X(Y) = X × 10^Y is the fractional abundance with respect to H₂

^aFrom Bockelée-Morvan et al., 2000 for comet Hale-Bopp at 1 AU, assuming H₂O/H₂=5×10⁻⁵

^bFrom Aikawa et al., 2003 (H₂CO), this thesis (HCN,H₂O), and Qi, 2001 (others)

^cFrom Bachiller et al., 1997 at position B2 assuming CO/H₂ = 10⁻⁴

^dFrom van Dishoeck & Blake, 1998 (and references cited); otherwise from Sutton et al., 1995

^eFrom Schöier et al. (2002) in the warm, dense inner part of the envelope \leq 150 AU in radius around IRAS 16293-2422

that the emitting region is in LTE was not strictly valid and produces an error of a factor of \sim 2 in the calculated column densities. These results were consistent with previous LVG calculations for LkCa 15 (van Zadelhoff et al., 2001) and support prior indications that the molecular line emission observed here arises from warm layers near the disk surface (Qi et al., 2003).

Although located a good distance from the star, these emission layers are kept relatively warm due to the flared disk geometry and direct stellar and scattered UV. This suggests that UV fields have a large impact on disk structure (and chemistry). In Chapter 3 CN, HCN and HCO⁺ were used as tracers of the effective UV field in several circumstellar disks. Although CN and HCN are produced in a similar manner, through reactions of N with neutral and ionic hydrocarbons, CN is destroyed through neutral-neutral reactions, while HCN is destroyed by ion-molecule chemistry and UV photolysis (to form CN). An increase in the effective UV field results in increased photoionization and photodissociation, which in turn leads to increased production of CN, HCN and HCO⁺. The increase in HCN production, however, is moderated by a coincident increase in HCN destruction, while the destruction rate of CN remains constant (or decreases). Observations of the CN/HCN ratio should therefore trace the strength of the effective UV field at disk surfaces, with increased CN/HCN corresponding to stronger UV fields. This has been found to be true in molecular clouds and photodissociation regions. Here, CN and HCO⁺ were found to be (at least weakly) correlated with tracers of the effective UV field; abundances of both molecules increased with increases in

the fractional IR luminosity and the dust settling parameter H/h . HCN, on the other hand, did not appear to be correlated with these or other disk parameters, likely due to the complexity of the reaction network for this molecule. Surprisingly, no molecular abundances appeared to be correlated with stellar parameters, such as L_* . This suggests that the interstellar radiation field may be more important than the stellar radiation field in the outer regions of disks ($R > 70$ AU) probed by these observations. HNC is produced and destroyed via ion-molecule reactions and thus is a very good probe of ion-molecule chemistry. Because it was only observed toward one source in our sample, a statistical analysis was not performed, but future studies may prove to be very valuable to the understanding of nitrogen chemistry in disks.

Deuterium fractionation has been observed to vary by 3 orders of magnitude between molecular clouds and the planets in our solar system. Thus, D/H ratios are a sensitive tracer of the conditions throughout the star formation process. Deuterium observations in the outer regions of disks are particularly interesting as a way to constrain the location and timescales of comet formation. In Chapter 4, we present the first detections of HDO and DCN toward circumstellar disks. The resulting deuterium fractionations in LkCa 15 and HD 163296 were found to be similar to those found toward the T Tauri star disk TW Hya and those observed in molecular clouds and hot cores.

The HDO emission presented in Chapter 4, as well as previous observations toward LkCa 15 (Qi et al., in prep), indicate large differences in the morphology of the emission in the integrated intensity maps (Figure ??). CO and HCO^+ emission peak at the source position while the HCN, CN and HDO emission peak approximately $2''$ away along the major axis of the disk. This is particularly interesting because the spectra for CO 2-1, HCO^+ , HDO and HCN do not differ significantly. Lack of emission toward the star results in only small changes to the line wings, which are often indistinguishable due to the noise in the spectrum. Clearly, imaging is necessary to study this type of disk structure and there is a need for detailed models which can be used to reproduce and interpret these images. For these reasons, we used the model described in Chapter 2, to simulate our observed channel maps and images of protoplanetary disks, first for the case of the emission for a telescope with infinite resolution and complete (u, v) coverage and then for the observed (u, v) coverage and resolution. We find that even with $2''$ resolution, the detailed disk structure is largely washed out by current observations and image deconvolution techniques.

The chemical models of Aikawa & Herbst (2001) and Willacy & Langer (2001) suggest that the radial distribution of HCN and CN in disks is determined by the processes of photodissociation by interstellar and stellar UV combined with desorption from grain surfaces. The newest models (Aikawa et al. 2002) suggest that the competition between interstellar and stellar UV in particular determine the variation in the amount of HCN as a function of radius. We simulate the emission morphology discussed above by concentrating the HCN in a ring around the star with an outer radius determined from the CO 2-1 observations (~ 430 AU) and an inner radius which is varied

to match the observed integrated intensity maps. These models can reproduce the structure of the HCN emission only with large depletion zones in the disk center ($R_i \sim 200\text{--}300$ AU). More realistic models will be used in the future to simulate the combined effects of desorption from grains and photodissociation of HCN from interstellar and stellar UV.

Although we have not yet modeled the HDO emission, the observed double peaked intensity map may also result from a ring-like distribution (or a steep outward gradient). Here models suggest that the annulus could be formed due to reduced production of HDO near the central star as H_2D^+ , the primary precursor to HDO, is created less efficiently due to the increasing temperature gradient in the inner disk. This causes the HDO abundance to peak at $R \approx 250$ AU (Aikawa & Herbst 2001). As the previous HCN models show, this morphology is consistent with the observed emission.

6.3 Grain composition and grain-surface chemistry

Current models of the chemistry in the outer regions of circumstellar disks (Willacy & Langer, 2000; Aikawa & Herbst, 2001), suggest that at large radii adsorption onto and desorption from grains can have a large effect on the gas-phase chemistry by removing (adding) molecules to (from) the gas. Additionally, due to the high mobility of hydrogen (and moderate mobility of C, N, S, and O), a higher degree of chemical complexity can be achieved on grain surfaces than in the gas phase and grains-surface chemistry is believed to play a critical role in the formation of pre-biotic molecules. The grain composition directly affects the extent of grain-molecule interactions (e.g., freezout onto grain surfaces) and resulting chemistry through molecule-to-grain binding energies and sticking coefficients. Recent models also indicate that disks are heated by the reprocessing of stellar radiation by grains near disk surfaces. This heating results in a flared geometry of the disk, with a cool midplane and warmer surface layer, and radiative transfer models (c.f. Chapter 2) suggest that it is these warm surface layers which are probed by the studies discussed above.

CO is the most abundant carbon-bearing species in the gas phase of the interstellar medium. It is also deposited very quickly on grain surfaces at high densities. Therefore, if prebiotic molecules are to be formed, the process must begin with the destruction of CO. If hydrogen is abundant on the grain surface, it will likely react with CO, possibly resulting in the formation of formaldehyde and methanol (Tielens & Whittet 1997). In the absence of large amounts of hydrogen on grain surfaces, oxygen may react with CO to form CO_2 , which can then be converted into formic acid. Formation of methanol and/or formic acid is necessary for the initialization of the formation of prebiotic molecules (Charnley et al., 1997). Thermal and energetic (UV/cosmic ray) processing of grains will likely determine the degree of chemical complexity in the grain-mantle ice. However, neither the exact dependence of the reactions above on these types of processing, nor the degree of processing of actual interstellar grains, have yet been determined.

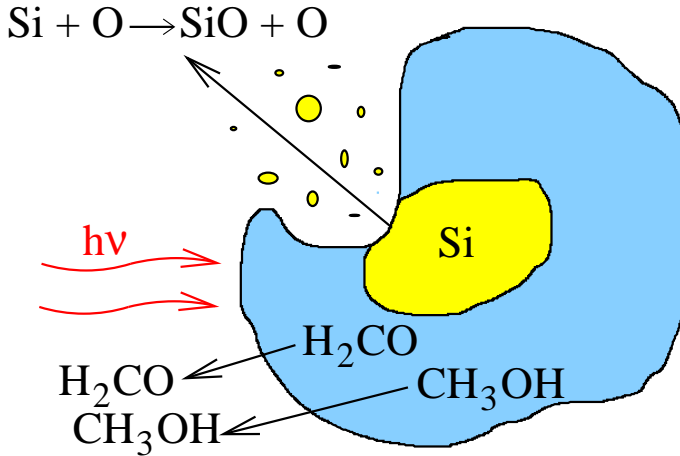


Figure 6.2 Dust processing. Exposure to high temperatures (>20 K for CO) or UV radiation leads to evaporation of the ices, and the influx of more complex molecules may stimulate gas-phase chemistry. In high-velocity environments (i.e., outflows), grain-grain collisions lead to sputtering, releasing grain core constituents into the gas phase, which leads to gas-phase production of molecules such as SiO.

The nature of grain mantle and coupled gas-grain chemistry has been extensively studied in the warm, dense hot cores around massive protostars (Charnley et al., 1997), but little is known about grain mantle processes in circumstellar disks. Accordingly, we have examined grain and grain surface chemistry through the observation of a few key species, namely, methanol, formaldehyde and silicon monoxide. These particular molecules have been widely observed in hot cores and their chemistry is fairly well understood. Both methanol and formaldehyde have been detected in the disks encircling the solar type stars LkCa 15 (Qi, 2001; Aikawa et al., 2003) and DM Tau (Dutrey et al., 1997) indicating the effectiveness of complex molecule formation on grains in disks (as well as hot cores) and a possible route to the in situ formation of pre-biotic molecules within the solar nebula through thermal and energetic (UV/cosmic ray) processing of grains. A summary of the LkCa 15 observations is shown in Figure 6.3. Because methanol and formaldehyde are formed on grain surfaces, they can desorb easily in warm environments and remain somewhat stable in the gas phase in the absence of ions (see Figure 6.2). In contrast, SiO is formed from grain interiors when silicon is released from grain cores through violent interactions of grains and is a tracer of more violent disk processing, such as occurs in shocks or outflows. SiO was searched for, but not detected toward LkCa 15; inferences on the turbidity of outer disks can be made from this result. The presence of methanol and formaldehyde in disks, indicates that the disk surrounding LkCa 15 is reasonably quiescent.

Sulfur chemistry is also used to trace the evolution of hot cores; atomic sulfur depletes onto grains surfaces (and can be converted into H₂S or OCS) due to low temperatures in the dense cloud core, evaporates in the hot core stage, and is rapidly converted to SO and SO₂, and more slowly into CS, in the gas phase. In this manner, the relative abundances of S-bearing molecules can be used as

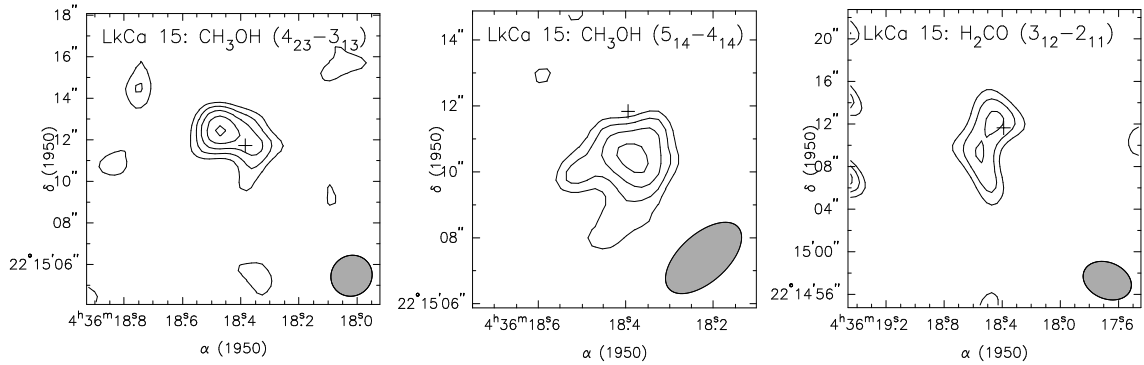


Figure 6.3 OVRO observations of formaldehyde and methanol toward T Tauri star LkCa 15 (Qi, 2001). The left and center panels show emission from CH₃OH and the right panel shows H₂CO emission. The H₂CO emission toward LkCa 15 is consistent with that observed at the Nobeyama Millimeter Array by Aikawa et al. (2003). Both molecules show emission which does not peak at the source position, similar to that observed for emission from other species in this disk.

a “chemical clock”, which measures the time since H₂S was released from grain surfaces (Hatchell et al., 1998). In the case of disks, the abundances of S-bearing molecules indicate the time since significant reprocessing of the grains has occurred. Toward LkCa 15 we observed large amounts of CS, including the isotope, C³⁴S (= [CS]/20), but no SO, SO₂, H₂S or OCS were detected (see Figure 6.4). The upper limits are only low enough to limit the abundances of these molecules to \sim [CS]. According to the models of Hatchell et al. (1998), comparable abundances of sulfur species indicate that this region of the disk is reasonably quiescent, which is consistent with the discussion of grain chemistry above. The fact that there is a lack of freshly desorbed H₂S may also suggest that the outer regions of disks are stratified, where the timescale for mixing between the observable layer and the layers where thermal desorption is occurring is longer than the chemical timescale for conversion of H₂S to CS.

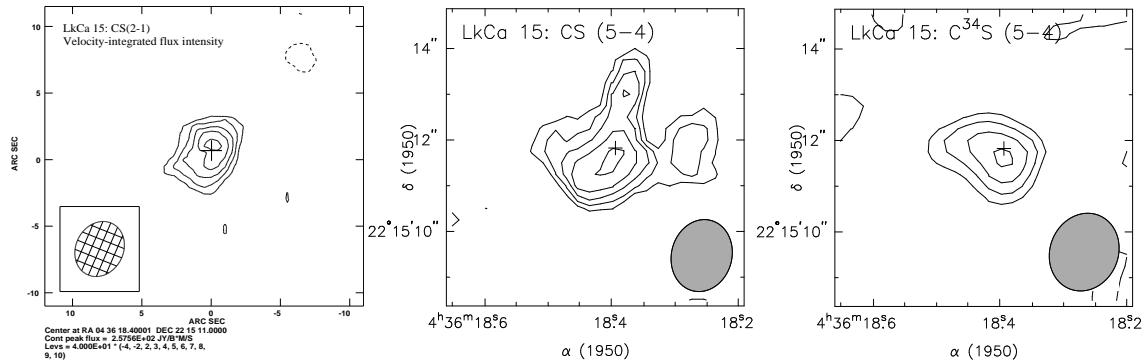


Figure 6.4 Observations of S-bearing molecules toward the protoplanetary disk around the T Tauri star LkCa 15 (Qi, 2001). From left to right, the panels show the CS 2-1, CS 5-4 and C³⁴S 5-4 emission.

As mentioned above, the dust composition can have large effects on the gas-phase chemistry

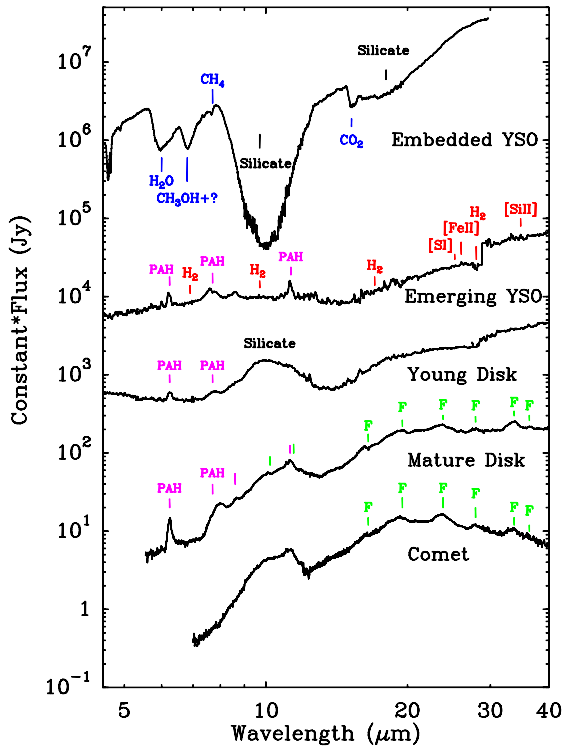


Figure 6.5 Evolution of IR spectra toward YSOs and comets (from Evans et al., 2003). The silicate feature changes from absorption of amorphous silicates in young, embedded protostars, to emission of amorphous and crystalline silicates in older disks and comets (F = forsterite).

and physical geometry of disks, and therefore knowledge of the dust composition is essential. Dust in early stages of star formation appears to be primarily amorphous silicates (Hanner et al., 1998). Observations of silicate emission in high-mass YSOs suggest an evolutionary sequence in which some of these amorphous silicates are crystallized during the star (and planet) formation process, resulting in the crystalline materials found in primitive solar system objects such as carbonaceous chondrites, comets and interplanetary dust particles (Figure 6.5). In Chapter 5, the 8–13 μm spectra were obtained for several low and intermediate mass YSOs. An evolutionary sequence from absorption in young, embedded sources, to emission in isolated stars and complete absence in older “debris” disks seen in ISO observations of high/intermediate-mass YSOs (Meeus & Waelkens, 1999) was confirmed and extended here to \sim solar mass stars. In contrast to the structured emission feature observed for most HAE stars, the shape of the silicate spectra of most T Tauri stars in our sample was very similar to that of the ISM and source-to-source variations in this shape are consistent with growth in the average size of the dust grains from 0.1–2 μm (van Boekel et al., 2003), with models of optically thin disks of amorphous silicate (>80%) dust whose geometries are similar to those predicted by

Dullemond (2002). The spectrum toward the T Tauri star Hen 3-600A *does* show emission typical of crystalline silicates (similar to the HAE star HD 179218 observed in our sample), indicating that under some conditions crystallization of silicates *can* occur in disks around *low mass* stars. The strength, but not the shape, of the emission features was found to be correlated with the fractional infrared luminosity (that is, the optical depth of the disk).

6.4 Future observations and models

As discussed in Chapter 5, the determination of the dust composition in disks around \sim solar mass has been limited by the sensitivity of current instrumentation; ISO studies of silicates were confined to intermediate or high-mass stars and ground based observations are restricted to the $10\ \mu\text{m}$ observing window. With the successful August 2003 launch of the Space Infrared Telescope Facility (SIRTF), much expanded studies, including disks around low mass, sun-like stars, can be expected creating a database analogous to ISO studies of high/intermediate-mass stars. Early SIRTF observations will include a large sample of low mass YSOs, ranging from embedded protostars to optically thin disks, via the combination of the Evans ($\tau_{dust} > 1$) and Meyer ($\tau_{dust} < 1$) Legacy Science programs (Evans et al., 2003; <http://febs.as.arizona.edu>), whose data will become publically available upon collection and pipeline reduction. Additionally, these studies will include observations of silicate emission features in the $15\text{--}40\ \mu\text{m}$ region, which are inaccessible from the ground and depend intricately on the coordination of the silicon atoms; thus providing more specific information about the minerals present, including the Mg/Fe ratio. The mineral content of the grains in each stage of evolution can thus be directly compared to that of meteorites, asteroids and comets. These studies will allow the crystallinity of the silicates in disks to be calculated, and the connections between disk temperatures and morphology (begun in Chapter 5), to be established through comparison of the amorphous/crystalline silicate ratios with indicators of disk flaring, such as the shape of the far IR excess (Chiang et al., 2001). In this manner, the ubiquity of cold crystalline silicates could be assessed and their formation mechanism can be explored through correlations with age or grain growth indicators.

Details of disk chemistry are most completely examined with high sensitivity, dynamic range and spatial resolution of interferometric studies of molecular species. CO emission and dust radiation has been observed for disks around many stars, but extensive chemical studies have been performed toward only a few T-Tauri star disks, including those presented in this thesis, LkCa 15, DM Tau, GG Tau and TW Hya (Qi, 2001; Dutrey et al., 1997; Kastner et al., 1997). Even for the brightest disks, millimeter arrays are not yet sensitive enough at high frequencies to reliably detect molecules with emission lines in the 1 mm region (i.e., H_2CO , CH_3OH , HDO) unless very long integration times are used. In the somewhat near future, a new generation of interferometers, including the Submillimeter

Array (SMA) and the Combined Array for Research in Millimeter-wave Astronomy (CARMA) will offer improved sensitivity ($\sim 5 \times$) over current arrays, enabling studies such as those discussed above to be more efficiently performed over larger samples. The improved sensitivity should also enable the detection of more weakly emitting species, such as prebiotic molecules, which have currently only been detected in hot cores. In the more distant future, the Atacama Large Millimeter Array (ALMA), will offer improvements in sensitivity by a factor of 20 over current arrays! Additionally, ALMA will be able to achieve a spatial resolution of $10^{-3}''$, which corresponds to ~ 0.1 AU for sources in nearby star-forming regions (at a distance of 140 pc). At this resolution, the planet-forming regions of disks can be probed and truly in situ measurements of the nebular chemistry will be possible for the first time.

Even before the advent of ALMA, molecular observations of circumstellar disks may be able to detect signatures of planet formation in progress, shedding light on the formation process. Although circumstellar disks have now been observed in the millimeter and infrared (as discussed above), and some of these disks are clearly old enough to possess large planetesimals or protoplanets, clear signatures of planet formation are difficult to observe. Accretion of a protoplanet of size greater than $\sim 10 M_E$ results in the formation of a gap in the disk, but models indicate the difficulty of detecting changes in the spectral energy distribution due to disk clearing (Wood et al., 2002, Steinacker & Henning, 2003) and direct imaging of gaps (Wolf et al., 2002) or rings of material disturbed by protoplanets (Ozernoy et al., 2000). To date, evidence for planet formation has only been observed in disks of reprocessed material around older stars. High-resolution IR imaging of the 20 Myr old, debris disk β Pictoris (Wahhaj 2003), shows evidence of four such rings, with orbits at 14, 29.1, 51 and 81 AU from the star. Structure seen in the emission from debris disks around ϵ Eridani and Vega have also been reproduced with models involving protoplanets, but the exact origin of the observed structure is unclear.

Observations of the chemistry in disks may be able to more selectively probe the planet formation process. After gap formation, material accretes onto the planet through narrow flows onto a circumplanetary disk with spiral density structure. The properties of the circumplanetary disk are very different from the circumstellar disk, resulting in a significant change in the chemistry. For example, NH₃ and CH₄ dominate in the circumplanetary disk, whereas N₂, HCN and CO dominate in the circumstellar disk. Additionally, NH₃ and CH₄ are the predominant species on grains and are released into the gas in the shocked regions, resulting in enhanced abundances of these species near the site of planet formation. The planet formation process may therefore be detectable through chemical tracers, such as CO/CH₄ and HCN/NH₃ ratios via infrared observations of CO/CH₄ and HCN/NH₃, using the line shape and the excitation of each transition to assign the observed density ratios with the circumplanetary disk. Such studies require high dynamic range, high spectral resolution observations to distinguish between emission from the circumstellar and circumplanetary disks,

and should be attainable with new instruments such as NIRSPEC at the Keck telescope, VISIR at the VLT and the EXES spectrograph on SOFIA.

As discussed in Chapter 2, radiative transfer modeling is essential for the interpretation of spectral line shapes and maps of molecular distributions of circumstellar disks. The application of such models in this thesis is but a preliminary step, and merely indicate the usefulness of combining radiative transfer models with standard imaging techniques to more closely simulate observed molecular distributions, such as those of HCN and HDO in LkCa 15. In the near future, we will expand the current model to include radial gradients in the abundance of these molecules and establish the slope of the gradient required to reproduce the observed emission. Fits will also be carried out in the (u, v) plane where rigorous error propagation enables detailed least squares fits to the observational data (see, for example, Dartois et al., 2003). These complexity of these computations are currently limited by computer processor speed and memory. In the not-so-distant future, the combination of accurate radiative transfer calculations with detailed models of disk chemistry will be possible, enabling the direct comparison, and thus the eventual convergence, of the predicted and observed molecular distributions.

Bibliography

- Aikawa, Y. & Herbst, E. 2001, A&A, 371, 1107
- Aikawa, Y., Momose, M., Thi, W., van Zadelhoff, G., Qi, C., Blake, G. A., & van Dishoeck, E. F. 2003, PASJ, 55, 11
- Aikawa, Y., van Zadelhoff, G. J., van Dishoeck, E. F., & Herbst, E. 2002, A&A, 386, 622
- Allamandola, L. J., Bernstein, M. P., Sanford, S. A., & Walker, R. L. 1999, Space Sci. Rev., 90, 219
- Bachiller, R., Forveille, T., Huggins, P. J., & Cox, P. 1997, A&A, 324, 1123
- Bauer, I., Finocchi, F., Duschl, W. J., Gail, H.-P., & Schloeder, J. P. 1997, A&A, 317, 273
- Bergin, E. A. & Langer, W. D. 1997, ApJ, 486, 316
- Bernstein, M. P., Sandford, S. A., Allamandola, L. J., & Chang, S. 1995, ApJ, 454, 327
- Bockelée-Morvan, D., Lis, D. C., Wink, J. E., Despois, D., Crovisier, J., Bachiller, R., Benford, D. J., Biver, N., Colom, P., Davies, J. K., Gérard, E., Germain, B., Houde, M., Mehringer, D., Moreno, R., Paubert, G., Phillips, T. G., & Rauer, H. 2000, A&A, 353, 1101
- Charnley, S. B., Rodgers, S. D., Butner, H. M., & Ehrenfreund, P. 2002, Earth Moon and Planets, 90, 349
- Charnley, S. B., Tielens, A. G. G. M., & Rodgers, S. D. 1997, ApJ, 482, 203
- Chiang, E. I., Joung, M. K., Creech-Eakman, M. J., Qi, C., Kessler, J. E., Blake, G. A., & van Dishoeck, E. F. 2001, ApJ, 547, 1077
- D'Alessio, P., Calvet, N., & Hartmann, L. 2001, ApJ, 553, 321
- Dartois, E., Dutrey, A., & Guilloteau, S. 2003, A&A, 399, 773
- Dullemond, C. P. 2002, A&A, 395, 853
- Dutrey, A., Guilloteau, S., & Guelin, M. 1997, A&A, 317, L55

- Evans, N. J., Allen, L. E., Blake, G. A., Boogert, A. C. A., Bourke, T., Harvey, P. M., Kessler, J. E., Koerner, D. W., Lee, C. W., Mundy, L. G., Myers, P. C., Padgett, D. L., Pontoppidan, K., Sargent, A. I., Stapelfeldt, K. R., van Dishoeck, E. F., Young, C. H., & Young, K. E. 2003, PASP, 115, 965
- Finocchi, F., Gail, H.-P., & Duschl, W. J. 1997, A&A, 325, 1264
- Hanner, M. S., Brooke, T. Y., & Tokunaga, A. T. 1998, ApJ, 502, 871
- Hatchell, J., Thompson, M. A., Millar, T. J., & MacDonald, G. H. 1998, A&A, 338, 713
- Hogerheijde, M. R. & van der Tak, F. F. S. 2000, A&A, 362, 697
- Hollis, J. M., Lovas, F. J., & Jewell, P. R. 2000, ApJ, 540, L107
- Kastner, J. H., Zuckerman, B., Weintraub, D. A., & Forveille, T. 1997, Science, 277, 67
- Kawaguchi, K., Ohishi, M., Ishikawa, S., & Kaifu, N. 1992, ApJ, 386, L51
- Meeus, G. & Waelkens, C. 1999, in ESA SP-427: The Universe as Seen by ISO, 373–+
- Ozernoy, L. M., Gorkavyi, N. N., Mather, J. C., & Taidakova, T. A. 2000, ApJ, 537, L147
- Qi, C. 2001, PhD thesis, California Institute of Technology
- Qi, C., Kessler, J. E., Koerner, D. W., Sargent, A. I., & Blake, G. A. 2003, ArXiv Astrophysics e-prints
- Schöier, F. L., Jørgensen, J. K., van Dishoeck, E. F., & Blake, G. A. 2002, A&A, 390, 1001
- Steinacker, J. & Henning, T. 2003, ApJ, 583, L35
- Sutton, E. C., Peng, R., Danchi, W. C., Jaminet, P. A., Sandell, G., & Russell, A. P. G. 1995, ApJS, 97, 455
- Takano, S., Masuda, A., Hirahara, Y., Suzuki, H., Ohishi, M., Ishikawa, S., Kaifu, N., Kasai, Y., Kawaguchi, K., & Wilson, T. L. 1998, A&A, 329, 1156
- van Boekel, R., Waters, L. B. F. M., Dominik, C., Bouwman, J., de Koter, A., Dullemond, C. P., & Paresce, F. 2003, A&A, 400, L21
- van Dishoeck, E. F. & Blake, G. A. 1998, ARA&A, 36, 317
- van Dishoeck, E. F., Blake, G. A., Jansen, D. J., & Groesbeck, T. D. 1995, ApJ, 447, 760
- van Zadelhoff, G.-J., van Dishoeck, E. F., Thi, W.-F., & Blake, G. A. 2001, A&A, 377, 566
- Willacy, K. & Langer, W. D. 2000, ApJ, 544, 903

Wolf, S., Gueth, F., Henning, T., & Kley, W. 2002, ApJ, 566, L97

Wood, K., Lada, C. J., Bjorkman, J. E., Kenyon, S. J., Whitney, B., & Wolff, M. J. 2002, ApJ, 567, 1183